International Journal of Research in Engineering and Science (IJRES)
ISSN (Online): 2320-9364, ISSN (Print): 2320-9356
www.ijres.org Volume 12 Issue 4 ǁ April 2024 ǁ PP. 25-40

Porosity variation and diagenetic evolution of Tipam Sandstone Formation of Geleki Oilfield of Upper Assam Basin

Bhargav Kashyap[1*], Pradip Borgohain[2], Yadav Krishna Gogoi[2], Manash Pratim Gogoi[2], Bubul Bharali[3]

[*1]*Department of Applied Geology, Dibrugarh University, Assam-786004, India*
[2]*Department of Petroleum Technology, Dibrugarh University, Assam-786004, India*
[3]*Department of Geology, Pachhunga University College, Aizawl, Mizoram 796001, India*
Corresponding Author: Bhargav Kashyap

Abstract
The present work is a comprehensive study to yield valuable insights into the diagenetic alterations causing porosity and permeability variations in the Tipam Sandstone Formation of Geleki oilfield. The characteristics of the clastic reservoirs are regulated by the frame work grains texture and different clay minerals present. Framework grains in the studied sandstones are mostly dominated by quartz with an adequate amount of feldspar and mica minerals. The diagenetic behavior of the sand samples was studied through an integrated analysis on megascopic, petrographic, X-ray diffraction (XRD) and scanning electron microscopy (SEM) examinations. Though sandstones are dominated by quartz grains, however, angularity of the grains, presence of substantial proportion of feldspars and matrix materials indicates that the sandstones are chemically immature to submature. Eventually, sand units become unstable and transform into secondary authigenic clays, which in turn deteriorate the reservoir characteristics. Mainly grain draping, pore bridging and pore filling clays, i.e., smectite, corrensite, illite and chlorite has affected the porosity of sand units of Tipam Formation. The correlation between permeability and porosity data shows how various clay minerals has significantly reduced the porosity, as well as the permeability, resulting in average porosity of 18% and permeability in the range of 40-100 mD respectively.

Keywords: *Diagenesis, Reservoir properties, Tipam Sandstone, Geleki oilfield*

Date of Submission: 21-03-2024 Date of acceptance: 03-04-2024

I. INTRODUCTION

The present study aims to unravel the primary and secondary porosities and diagenetic changes incurred after the deposition of Tipam Sandstone (Miocene) Formation of Geleki Oilfield of Upper Assam basin (Fig. 1). The Tipam Sandstone Formation is the bottom most unit of Tipam Group, which is subdivided into three formations from bottom to top viz. Tipam Formation, Girujan Clay Formation, and Nazira Sandstone in Geleki Oilfield of upper Assam basin. There are in total six numbers of hydrocarbon producing sands within the Tipam Sandstone Formation. The bottom three sands TS-6, TS-5 & TS-4 belong to Geleki Sandstone Member while the upper three sand horizons viz. TS-3, TS-2 & TS-1 belong to Lakwa Sandstone Member (Table 1). The Tipam Sandstone Formation dominantly consists of sandstone with subordinate siltstone and clay. The absence of coal and carbonaceous shale in sand units from TS-1 to TS-3 of Lakwa Member suggests the deposition of these sediments in a braided fluvial system. The TS-4 reservoir is deposited as a channel fill within Lower Clay Marker (LCM). The LCM is correlated over the entire North Assam Shelf area with huge variation in its thickness. It represents flood-plain-fluvial channel and over bank deposits of meandering fluvial systems. The Geleki oilfield is situated close to the Naga thrust belt at the southeastern point of the Upper Assam Shelf. It is thought that the majority of Geleki's structure is concealed beneath the Naga thrust. The Geleki structure is a twofold plunging anticline with a span of about 27 km^2 and has a NNE-SSW direction. In the Geleki oilfield, the first hydrocarbon was discovered in 1968. Although the primary focus of exploration was on Tipam (Miocene) and Barail (Oligocene) Group of rocks, however, few wells have also been completed in Kopili (Eocene) Formation. It has been reported that due to reservoir heterogeneity the productivity of hydrocarbons from the Tipam Sandstone Formation shows variations from horizons to horizons within the oilfield. Keeping this view in mind an attempt has been made, in the present study, to evaluate the diagentic alterations experienced by the rock and their impact on the reservoir properties of Tipam sandstones of Geleki oilfield. Megascopic,

petrographic, X-ray diffraction (XRD) and scanning electron microscopy (SEM) analysis have been conducted on the core and cutting samples of all the sands from TS-1 to TS-6.

II. MATERIALS & METHODS

In the study following data inputs were considered

2.1 Megascopic Analysis

Megascopic analyses of samples have been carried out based on core study using hand-held lens and stereo microscope. The study focused upon identifying the textural attributes and gross reservoir characters of the rock.

2.2 Rock Thin Section Analysis

For rock thin section analysis, selected drill core and cutting samples from Tipam Sandstone Formation of Geleki Oilfield has been considered. The thin sections were studied under Olympus Polarizing Microscope Model CX31P with Motic Image Analyser.

2.3 SEM (Scanning Electron Microscope) Analysis

Samples from key wells were taken into consideration for carrying out SEM analysis for reservoir petrography and identification of clays. The SEM photo-micrographs - the secondary electron images of sample are taken with JEOL JSM-7610F Field Emission Scanning Electron Microscope (FESEM) operating at 15KV to bring out the desired features. Energy Dispersive X-ray Spectroscopy (EDS), an analytical capability coupled with SEM provides elemental analysis on areas, as small as nanometers in diameter is also utilized during the study. The impact of the electron beam on the sample produces X-rays that are characteristic of the elements present on the sample. The EDS analysis helps in phase identification and in generating the elemental maps. These outputs, in turn, help in predicting the mineralogy of samples and also in confirming the XRD based mineralogy.

2.4 X-Ray Diffraction (XRD) Analysis

Using the X-Ray Diffraction (XRD) technology, samples from distinct wells that penetrated all of the sand units of the Tipam Formation, from TS-1 to TS-6, were examined for their mineral composition. The sample is powdered to 300 mesh using Fritsch Micro Pulverisette-7 machine. For bulk mineralogical analysis the powdered sample is scanned directly using Rigaku X-Ray. The method suggested by diffractometer (Model Ultima-IV with Ni-filtered Cu Kά radiation) with 2Ɵ ranging from 3º to 60º. The diffractogram, so generated, is a plot of 2θ vs Intensity and is interpreted by Reference Intensity Ratio (RIR) method with the help of standard reference patterns provided by International Centre for Diffraction Data (ICDD). Such interpretation is used to identify the constituent minerals of powdered sample of reservoir rock along with a semi-quantitative estimation of their bulk abundance in the sample.

III.RESULTS AND DISCUSSIONS

3.1Megascopic analysis

The samples of sand units from TS-1 to TS-6, as determined by megascopic analysis, have a grain sorting that ranges from poor to moderate, and their grained characteristics are sub-angular to sub-rounded. The sand samples show tight to moderate amount of grain packing. With a sufficient quantity of mica and plagioclase-feldspar minerals, quartz predominates in the framework grains of sandstone samples. However, in TS-2 sand samples of wells A-12 & A-105 and TS-1 sample of well A-95 are having good sorting of grains (Fig. 2a, 2b & 2c).

3.2Petrographic analysis (Microfacies Analysis)

The sandstones are fine to medium grained, constituting of quartz (58%-75%), feldspar (10-20%) and rock-fragments (10-15%) along with cements and matrix. Both monocrystalline (Fig. 3a) and polycrystalline (Fig. 3b) varieties of quartz grains are observed. Palgioclase feldspar (Fig. 3c) is found dominating over k-feldspars. Igneous, sedimentary and low to medium grade metamorphic rock fragments are recorded (Fig. 3d, 3e & 3f). Chert grains are also commonly recorded within the sandstone (Fig. 3g). Micas (Fig. 3h) are relatively smaller than framework grains in the rock. The sandstones are mainly sub-litharenite (Fig. 3i) to sub-arkose (Fig. 3j). The presence of concavo-convex and sutured grain (Fig. 3k) contacts indicates that the Tipam Sandstones have undergone mechanical compaction due to the pressure of overlying strata. The mechanical compaction of sediments is witnessed by bending of detrital mica flakes, fracturing of quartz, feldspar and rock fragments (Fig. 3h, 3l). The compaction brings the grains into closer contacts along long or concavo-convex boundaries. Certain grains show sutured contacts indicating pressure solution effects. The silica solutions

released from these contacts passes through the pore spaces and then precipitate over the quartz surfaces as overgrowths [8]. These overgrowths (Fig. 3m) reduce the primary porosity within the rock. The impregnated rock- thin section analysis shows an average porosity value of 18% (Fig. 3n). Certain samples show floating texture wherein calcite cement (Fig. 3o) is dominating over others. Relatively high amount of plagioclase feldspar and mica minerals makes these sand units chemically immature and unstable. Due to circulation of pore fluids during burial diagenesis, the feldspar grains are altered to clay minerals (Fig. 3p). Grain surfaces of present study exhibit dull luster due to presence of such type of clay coatings. Fractured quartz grains are frequently observed within the rock which may be due to the overburden compaction effects as well as the tectonic effects of the nearby Naga thrust of Schuppen belt. Grain dissolution and corrosion (Fig. 3q) has also been recorded. This feature enhances the reservoir quality of the rock [10]. The shale clasts and low-grade metamorphic rock fragments are observed to convert to pseudo matrix due to deformation (Fig. 3r), which reduces the porosity and permeability of the rocks [4].

3.3 SEM Analysis:

Cutting and core samples of TS-1, TS-2, TS-4, TS-5 & TS-6 sands of Tipam Formation from North Geleki field and main Geleki field have been examined under Field Emission Scanning Electron Microscope (FESEM) for the identification of rock texture, surface morphology, authigenic components, particularly clay minerals and better visualization of pore geometry and pore-filling minerals. The study was further aided by EDS analysis of interesting areas within sample to know the elemental compositions to interpret mineralogy. The study reveals that sand units are moderately hard, compacted, moderately sorted and moderately packed sandstone, composed of sub-angular to angular and sub-rounded quartz, plagioclase-feldspar, micas, etc. SEM study further, shows that the illite, montmorillonite, smectite, corrensite and chlorite precipitated as pore bridging and grain draping clays (Fig. 4, 5). Though primary intergranular pore spaces with fair connectively are seen at places (Fig. 4), however, sorting, grain packing and growth of pore bridging and draping clays tend to reduce porosity and connectivity. Secondary micro-pores developed due to intragranular fracturing and partial dissolution of framework grains have been observed. However, in certain samples, these secondary pore spaces are again filled up by authigenic clay minerals. Authigenic chlorite, illite, and corrensite/smectite with occasional presence of mixed layer illite-chlorite clays are seen. Calcareous cement has been depicted by EDS analysis. Sand unit show well preserved primary intergranular pore spaces (Fig. 4, 5).

3.4 XRD Analysis

The XRD analysis reveals that the felsic minerals such as quartz, plagioclase and k-feldspars and micas are main framework minerals present in the studied sandstones. Pore bridging clay minerals like chlorite, smectite, corrensite, kaolinite, illite, and few amount of glauconite and mixed layer clays such as smectite-kaolinite, chlorite-montmorillonite, illite-montmorillonite are also present. Heavy minerals ilmenite, siderite, pyrite, limonite and rutile are observed in few samples. Carbonates minerals such as calcite and dolomite are present along with evaporite minerals like gypsum and barite (Table 2). The semi-quantitative distribution of bulk and clay minerals in the sample and X-ray diffractogram of Cutting / core sample of well A-12 and well A-15 are shown in Fig. 6 & Fig. 7.

3.5. Major Findings

3.5.1Diagenetic Evolution:

Inter-formational composition and its participation in post depositional mechanical and chemical processes can cause significant heterogeneity in sandstone reservoir quality [2]. The diagenetic processes affecting the present studied sandstones are precipitation of cement, mechanical compaction, grain deformation, fracturing, dissolution and replacement, recrystallization, and authigenesis. Study shows that ferruginous cements precipitated under reducing depositional settings after the first-generation cement was mechanically infiltrated by clay. Authigenic illite and mixed layer clay precipitation occurs after overgrowths of quartz and kaolinite. These clays appear as rims around detrital grains, reducing porosity and permeability. When sediments are buried, compaction of the sediments begins and gradually increases with depth. Fracturing of framework grains as well as the bending of detrital mica flakes (Fig. 3h), are signs of the mechanical compaction of sediments [1] The grains come into closer contact as a result of the compaction. The compaction brings the grains into closer contacts along long or concavo-convex boundaries further, on pressure solution forms to sutured contacts. According to [3], in typical circumstances, point or tangential contacts indicate an early diagenesis burial stage, while grain contact boundaries develop long and concavo-convex under deep burial stages with increased overburden load. Blatt also pointed out that at deeper burial depths, the buried loaded sand may contain a significantly higher proportion of longer, closer, concavo-convex, and sutured grain contacts. Long, concavo-convex contacts and the precipitation of clays or chert are indicators of the second stage of diagenesis, or locomorphic stage, of diagenesis [6]. The uniform covering of clays causes the lustre of

grain surfaces to be dulled. Most of these authigenic clays are formed as a result of direct precipitation from circulating pore fluid during burial diagenesis. Grain draping, pore bridging, and pore filling clays are primarily identified as smectite, corrensite, illite, and chlorite. Clay precipitation damages the connection by shrinking pore throats and converting the previously interconnected granular pore spaces into isolated pores. The process of chemical precipitation of pore solutions, which results in subsequent quartz overgrowths, is what causes cementation. The sandstones have undergone the first stage of diagenesis, or the telegenetic stage, if overgrowth in the quartz grains and replacement, dissolution, and corrosion of the grains by cements are present [11]. The silica cement, which is present in the studied sandstones as quartz overgrowth, influences the sandstone's reservoir quality (Fig. 3m). The low-grade metamorphic rock fragments are squeezed to generate a dispersed pseudo-matrix. In the sandstones under investigation, one of the significant diagnostic alterations that have been repeatedly noted is the partial replacement and dissolution of the framework grains by the cementing elements. Along the edges of the grains, quartz is replaced. The reservoir sand's porosity is improved by these replenishment procedures. Authigenic development of mica (right bottom mica grain of Fig. 3d) at the expenses of argillaceous matrix, at phyllomorphic stage of diagenesis, observed in the sandstones, may contribute to a decrease in the sandstone's porosity and permeability [5].

3.5.1 Porosity and Permeability Variations

Mainly smectite, corrensite, illite and chlorite are identified as grain draping, pore bridging and pore filling clays. Grains draping clays grow as pore bridging & filling clays and seal the intergranular areas of the rock. Precipitation of clays transform the well-connected inter granular pore spaces into isolated pores and shrink pore throats which damage the connectivity in the reservoir. Presence of smectite, corrensite, illite and chlorite clays has significantly reduced the porosity, as well as the permeability, resulting in average porosity of 18% and permeability in the range of 40-100 mD respectively. A wide variation in permeability in different wells indicating that there is lateral heterogeneity resulting in different reservoir quality in the same sand. Petrographic and mineralogical studies of cuttings and core samples depicts moderate to poor reservoir characteristics of Tipam pay sands.

IV.CONCLUSION

The studied sandstones are characterized by fine to medium grained, sub-angular to sub-rounded with moderate to poorly sorted texture. However, TS-2 and TS-1 sand units show good sorting as well as porosity in comparison to the other sand units. The packing of grains appears to be tight to moderate. Framework grains are mostly dominated by quartz with an adequate amount of feldspar, lithic fragments and mica minerals. The sandstones have experienced different types of digenetic alterations throughout its life cycle. Conversion of sedimentary and low grade metamorphic lithic fragments into pseudomatrix under the compactional effects and thereafter squeezing of constituent grains of the lithic fragments into intergranular pore spaces damages their intergranular pore connectivity. Such alterations have reduced the porosity of the rock. Further, relatively high amount of plagioclase-feldspar and mica minerals make these pay sands chemically immature. Feldspar grains are found altered to authigenic clays through diagentic alterations. Most of these authigenic clays are formed as a result of direct precipitation from circulating pore fluid during burial diagenesis. Such precipitation of clays transforms the well-connected inter granular pore spaces into isolated pores and shrink pore throats which damage the connectivity in the reservoir. The angularity of the framework grains and quartz overgrowth are also responsible for porosity reduction within the rock. Authigenic development of mica at the expense of argillaceous matrix and cements reduces the porosity. However, there are certain other alterations, which have made the studied sandstones good reservoirs by enhancing porosity and permeability. Intragnular fracturing, partial dissolution of framework grains, precipitation of clays over large quartz surfaces and thereby inhibiting overgrowths are some of the important diagenetic changes that have made the sandstones good reservoir by preserving primary porosity as well as generating secondary porosity. However, presence of smectite, corrensite, illite and chlorite clays have significantly reduced the porosity, as well as the permeability, resulting in average porosity of 18% and permeability in the range of 40-100 mD respectively.

REFERENCES

[1]. Bharali, B. and Borgohain, P. (2013): Few characteristics of Tipam Sandstone Formation within oilfield areas of Upper Assam – A study based on wireline log data. Jour. of Earth. Sci., Special Volume, Dept. of Applied Geology, Dibrugarh University, pp.36-45.
[2]. Bhuyan, D., Borgohain, P. and Bezbaruah, D. (2022) Diagenesis and Reservoir Quality of Oligocene Barail Group of Upper Assam Shelf, Assam and Assam Arakan basin, India. Jour. Asian Earth Sci., v.7, pp.1-13, doi:10.1016/j.jaesx.2022.100100
[3]. Blatt, H. and Christie, J.M. (1963): Undulatory extinction in quartz of igneous and metamorphic rocks and its significance in provenance study of sedimentary rocks. Journal of Sedimentary Petrology, v.33, pp.559-579.
[4]. Borgohain, K., Borgohain, P., Bharali, B. and Baruah, J. (2019) Sedimentological characteristics of the barail arenaceous unit of makum north Hapjan oil field, Assam. Internat. Jour. Earth Sci. Geol., v.1(2), pp.66-73. DOI:10.18689/ijeg-1000108

[5]. Borgohain, P., Bezbaruah, D., Gogoi M. P., Gogoi, Y.K., Phukan, P.P., Bhuyan D., (2019) Petrography and diagenetic evolution of the Barail sandstones of Naga Schuppen belt, North East India: implication towards reservoir quality. Current Science, VOL. 121, NO. 8, 25 October 2021. doi: 10.18520/cs/v121/i8/1107-1113
[6]. Dapples, C. E., (1967): Diagenesis of Sandstones. In: G. Larsen and V. G.Chillinger (eds.), Diagenesis of Sediments. Elsevier Publishing Company, New York, pp.91-125.
[7]. Deshpande, S.V., Goel, S.M., Bhandari, A., Baruah, R.M., Deshpande, J.S., Kumar, A., Rana, K.S., Chitrao, A.M., Giridhar, M., Chowdhuri, D., Kale, A.S., Phor, L., 1993. Lithostratigraphy of Indian Petroliferous Basins: Unpublished Report of ONGC.
[8]. Gogoi, M. P., Borgohain, P., Gogoi, Y. K., Bezbaruah, D., (2023): Petrography, Diagenesis and Hydrocarbon Source Potential of the Barail and Disang Group of Rocks in Parts of the Naga Schuppen Belt and Inner Fold Belt of Assam-Arakan Basin. Jour. Geol. Soc. India (2023) 99:906-916 https://doi.org/10.1007/s12594-023-2412-z
[9]. Naidu, B.D. and Panda, B.K. (1997): Regional source rock mapping in upper Assam Shelf, in Proceedings of the Second International Petroleum Conference and Exhibition, Petrotech-97: New Delhi, v. 1, p. 350–364.
[10]. Saikia, G. and Borgohain, P. 2013. Petrography and Sandstone Chemistry of Oil Bearing Tipam Sandstone Formation in Parts of Upper Assam Shelf. Journal of Earth Science, Special Volume, 95-105.
[11]. Sengupta, S. (1994): Introduction to Sedimentology. Oxford & IBH Publishing Co. Pvt. Ltd. India.

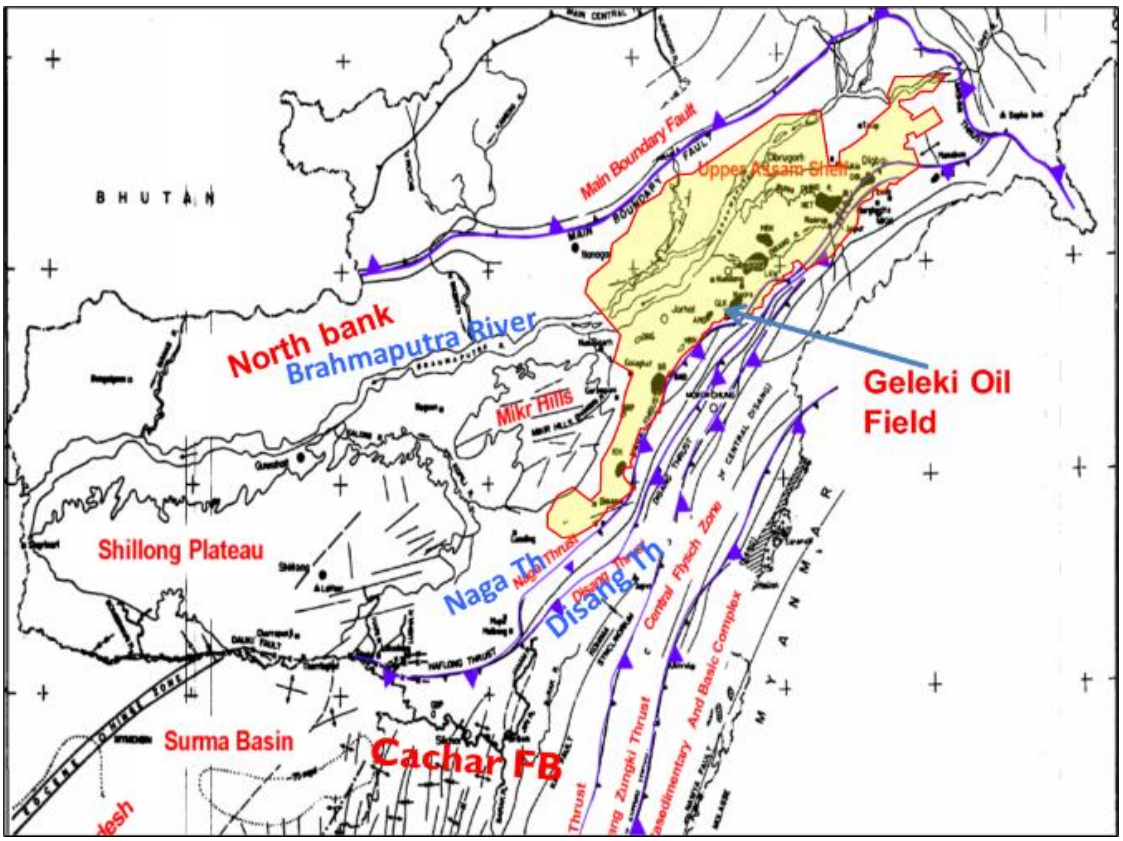

Fig. 1: Oil and gas fields in Assam province showing study area (Geleki oilfield) [9]

Table 1: The generalized stratigraphy of the shelf area [7].

GENERALISED STRATIGRAPHIC SUCCESSION IN UPPER ASSAM SHELF (UPPER ASSAM NORTH SHELF)					
AGE		**THICKNESS (m)**	**GROUP**	**FORMATION**	**LITHOLOGICAL DESCRIPTION**
Neogene	Recent-Pleistocene	600-1200		Alluvium	Unconsolidated sands with gravel, silt and minor clays
	Pleistocene to Pliocene	150-1000	Mora n	Dhekiajuli	Thickly bedded sands with minor clays
		250-550		Namsang	Intercalated sands and mottled clay
	Pliocene – Miocene	20-580	Tipam	Nazira Sst	Predominantly sandstone with minor clays
		50-850		Girujan	Mottled and variegated clays with intercalations of silt/sandstone beds
		160-550		Lakwa Sst. (TS1-TS2-TS3) (Tipam Formation)	Massive sandstone with clay/shale alternations
		200-400		Geleki Sst. (LCM+TS4-TS5-TS6) (Tipam Formation)	Massive sandstone with clay/shale alternations with minor calcareous matter in the lower part.
				Safrai	Conglomerate/ grit topped by sandstone shale alternations.
Paleogene	Oligocene – Late Eocene	40-500	Barail	Rudrasagar	Carbonaceous shale and coal with alternations of sand & shale.
		80-250		Demalgaon	Dominantly sandstone with intercalations of minor shale
		40-350		Disangmukh	Carbonaceous shale and sand alternations.
	Late Eocene-Late Paleocene	100-450	Jaintia	Kopili	Dominantly shale with sandstone beds
		50-120		Sylhet	Mainly limestone with shale/sand alternations
		10-35		Tura	Weathered granitic wash, fine to coarse grained sand with kaolinite clay, coal and shale
Precambrian		Granitic Basement			Granite and Gneissic Complex.

Fig. 2a: Well A-12, TS-2 sand unit, Core Sample

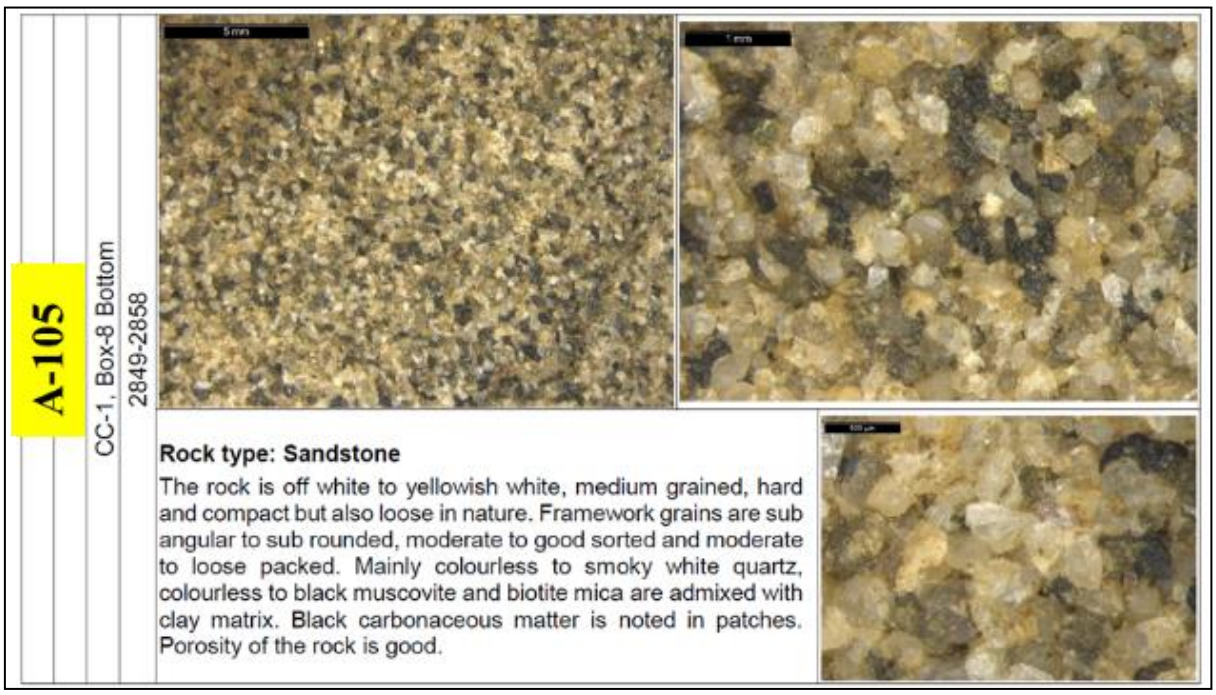

Fig. 2b: Well A-105, TS-2 sand unit, Core Sample

Rock type: Sandstone

The rock is off-white, medium sand grained, hard and compact to loose in nature. Non-calcareous. Framework grains are sub angular to sub rounded, moderate to fair sorted and moderate packed. Mainly colourless to smoky white and pink quartz, muscovite and biotite mica, white to light grey feldspars are admixed with clay matrix. Grains are coated with clay. Visual Porosity of the rock is moderate. Intergranular porosity can be observed and filled up by clay matter. Connectivity seems poor.

Fig. 2c: Well A-95, TS-1 sand unit, Core Sample

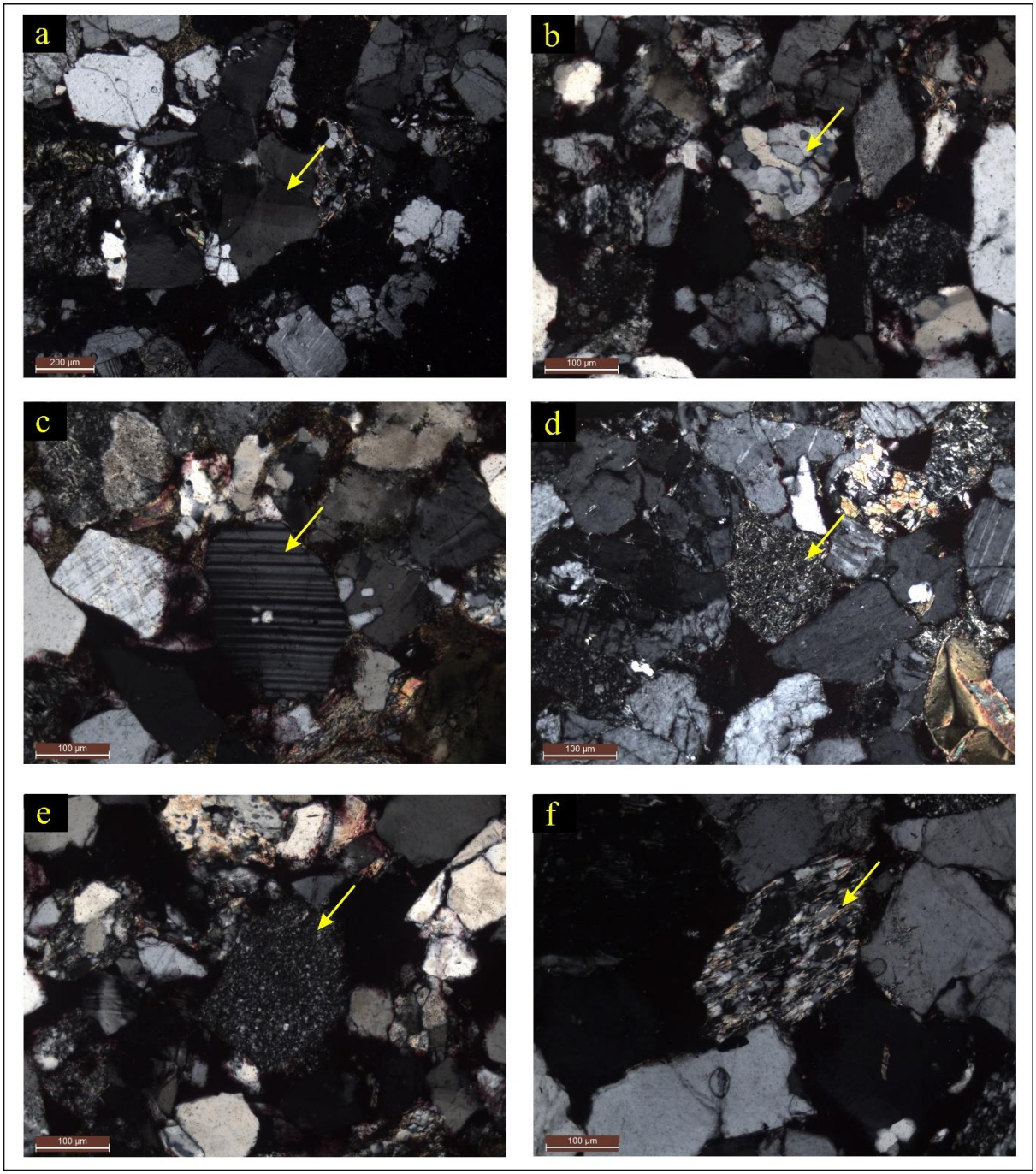

Fig. 3: a) Monocrystalline Quartz, b) Polycrystalline Quartz, c) Plagioclase Feldspar, d) Igneous Rock Fragment, e) Sedimentary Rock Fragment and f) Metamorphic Rock Fragment.

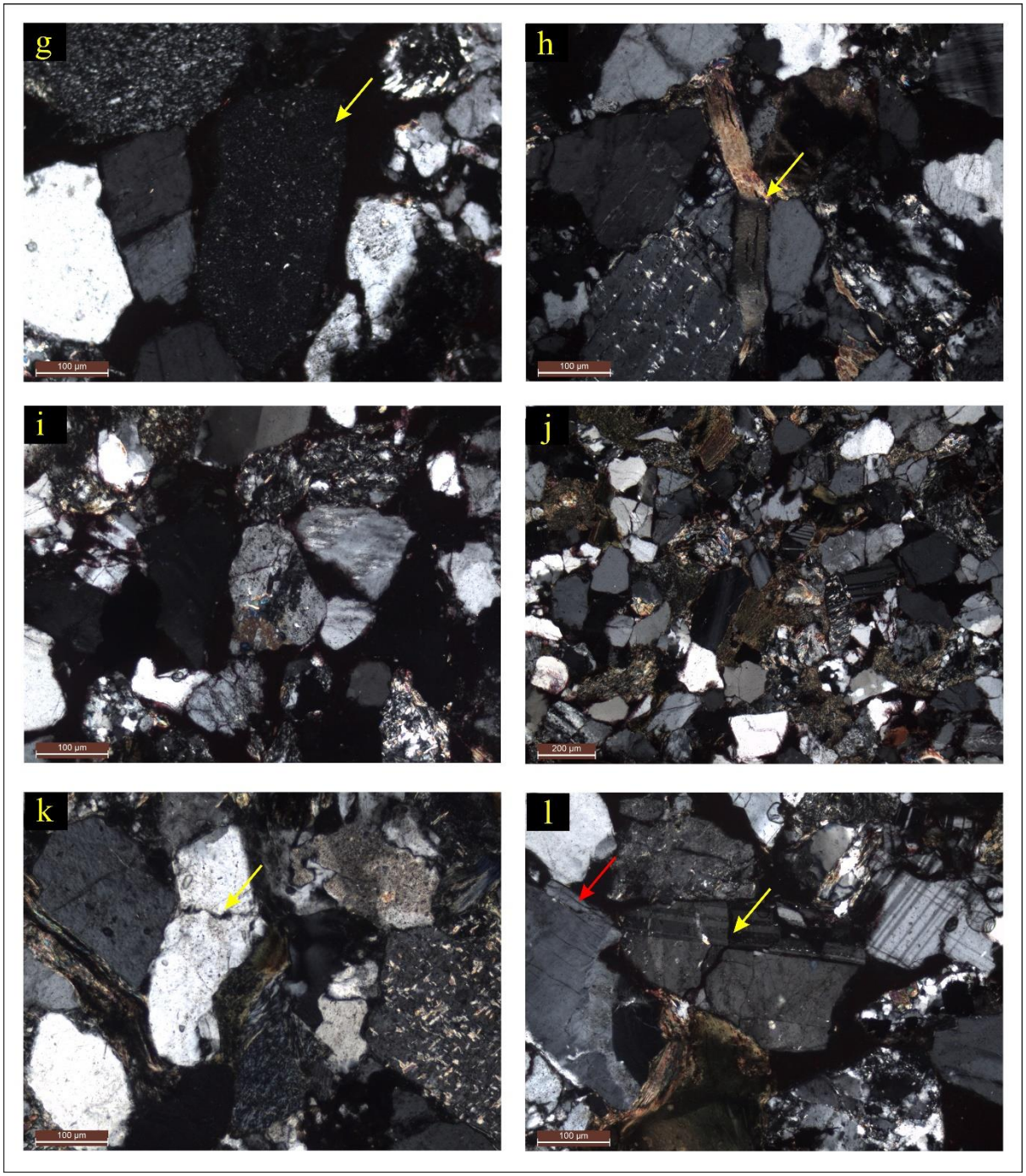

Fig. 3: g) Chert, h) Bending of Mica, i) Sublith Arenitic Sandstone, j) Sub-Arkosic Sandstone, k) Sutured contact between Quartz grains, l) Fractured Quartz (red arrow) and Plagioclase Feldspar (yellow arrow).

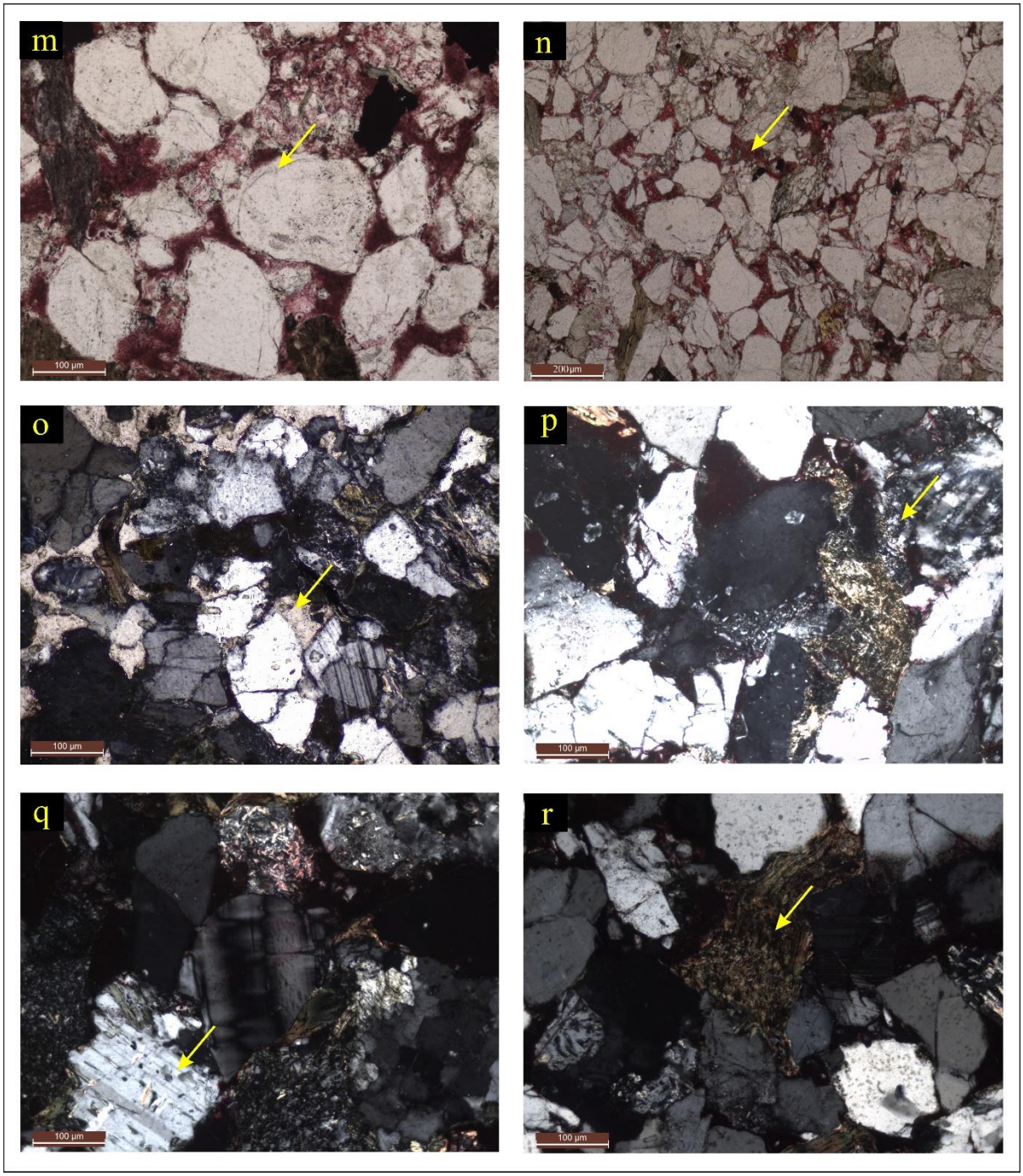

Fig. 3: m) Quartz overgrowth, n) Impregnated sandstone with red dye showing pore spaces between framework grains, o) Calcite cement, p) Alternation of Feldspar into clay minerals, q) Surface corrosion of Plagioclase Feldspar and r) Pseudo-matrix.

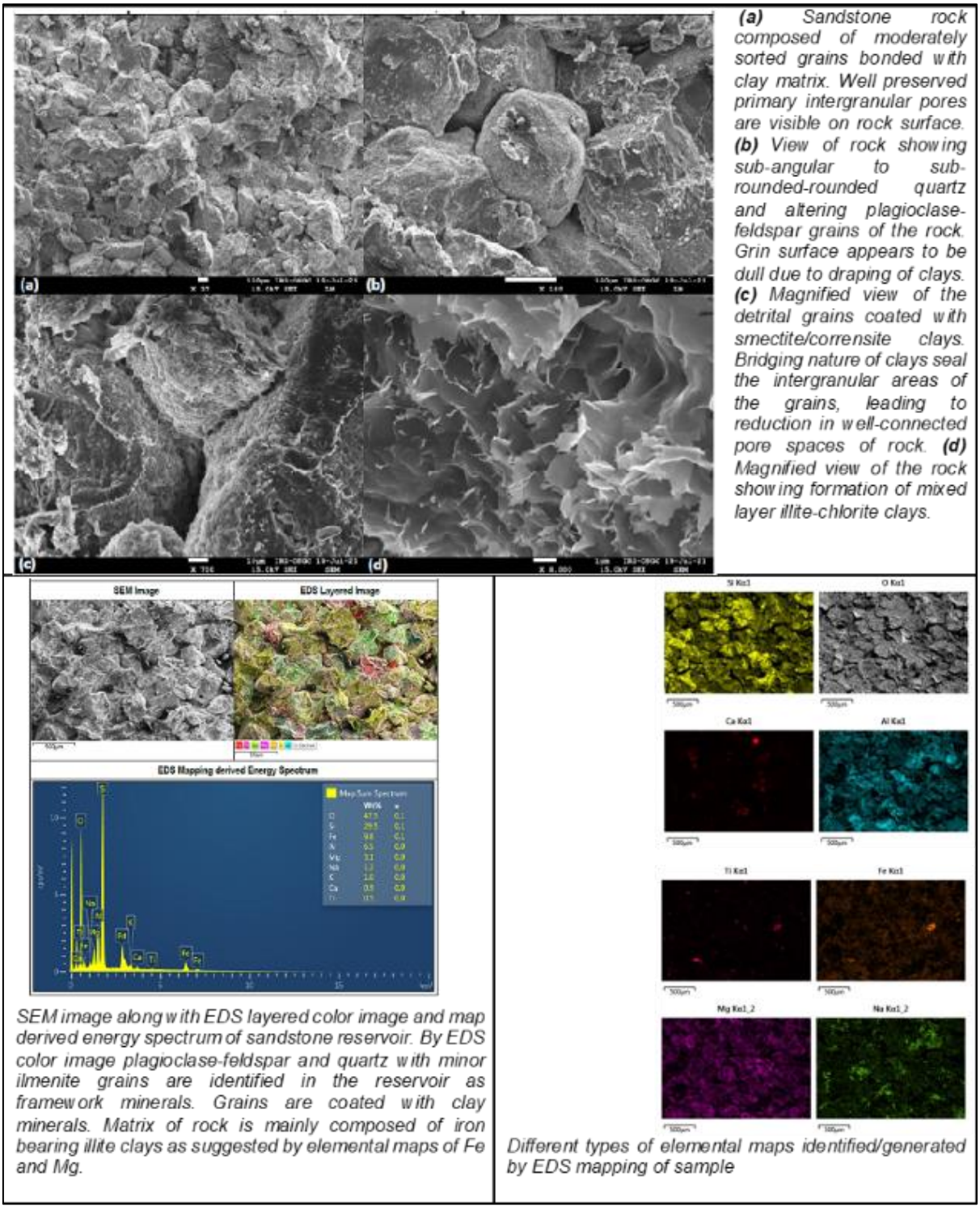

(a) *Sandstone rock composed of moderately sorted grains bonded with clay matrix. Well preserved primary intergranular pores are visible on rock surface.* ***(b)*** *View of rock showing sub-angular to sub-rounded-rounded quartz and altering plagioclase-feldspar grains of the rock. Grin surface appears to be dull due to draping of clays.* ***(c)*** *Magnified view of the detrital grains coated with smectite/corrensite clays. Bridging nature of clays seal the intergranular areas of the grains, leading to reduction in well-connected pore spaces of rock.* ***(d)*** *Magnified view of the rock showing formation of mixed layer illite-chlorite clays.*

SEM image along with EDS layered color image and map derived energy spectrum of sandstone reservoir. By EDS color image plagioclase-feldspar and quartz with minor ilmenite grains are identified in the reservoir as framework minerals. Grains are coated with clay minerals. Matrix of rock is mainly composed of iron bearing illite clays as suggested by elemental maps of Fe and Mg.

Different types of elemental maps identified/generated by EDS mapping of sample

Fig. 4: SEM image of Well A-12, TS-2 sand unit

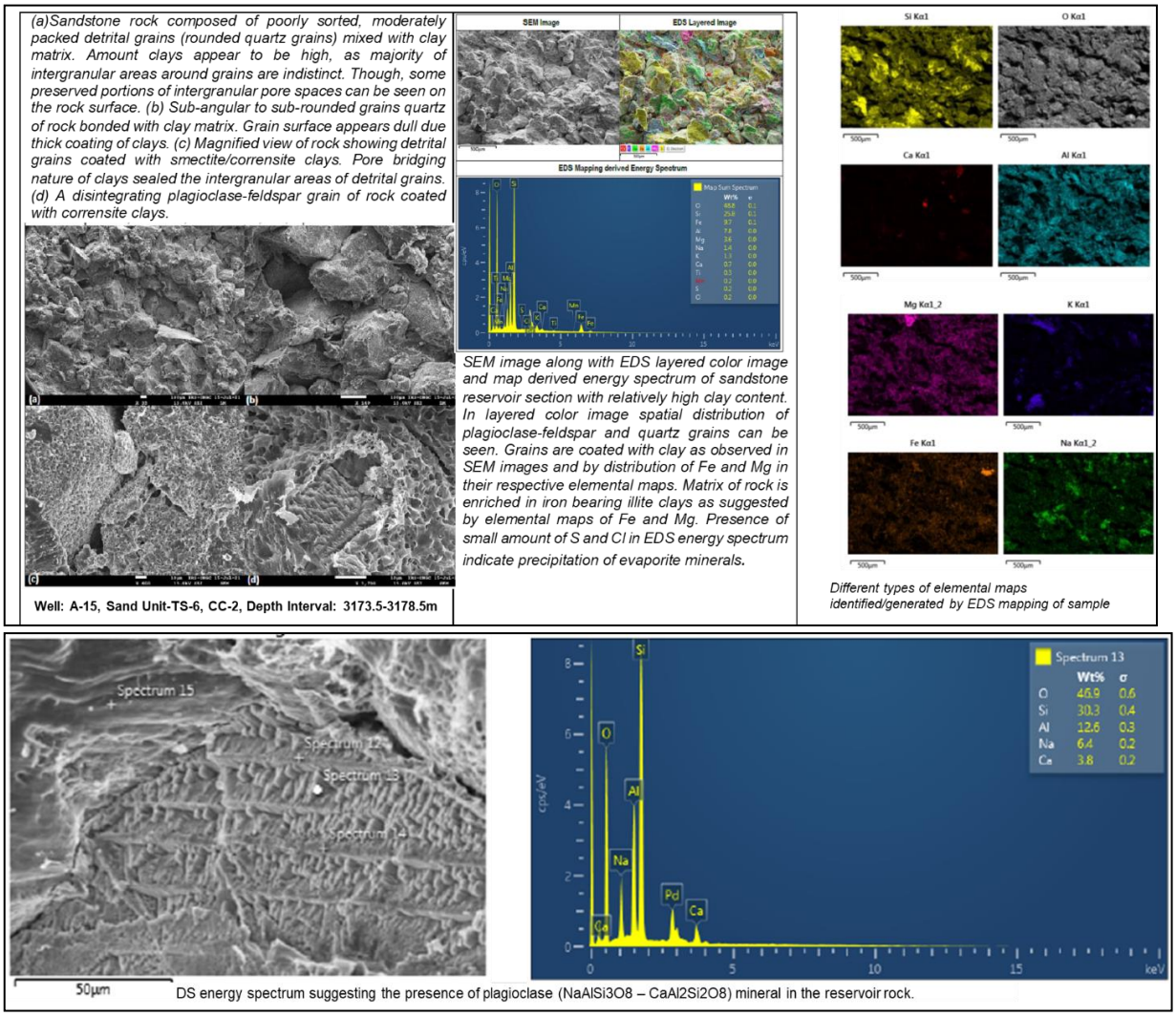

Fig. 5: SEM image of Well A-15, TS-6 sand unit

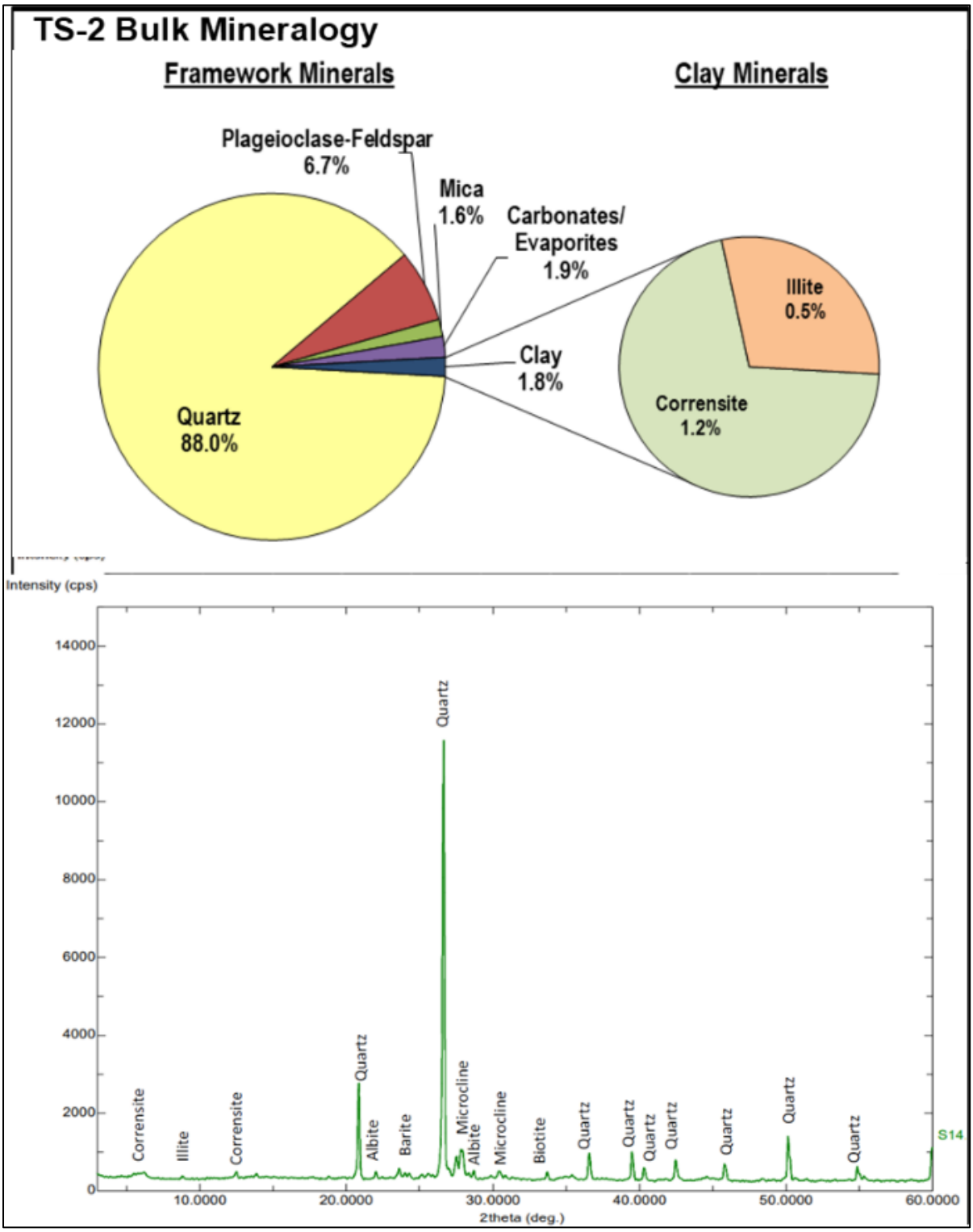

Fig. 6: The semi-quantitative distribution of bulk and clay minerals in the sample and X-ray diffractogram of Cutting / core sample well A-12

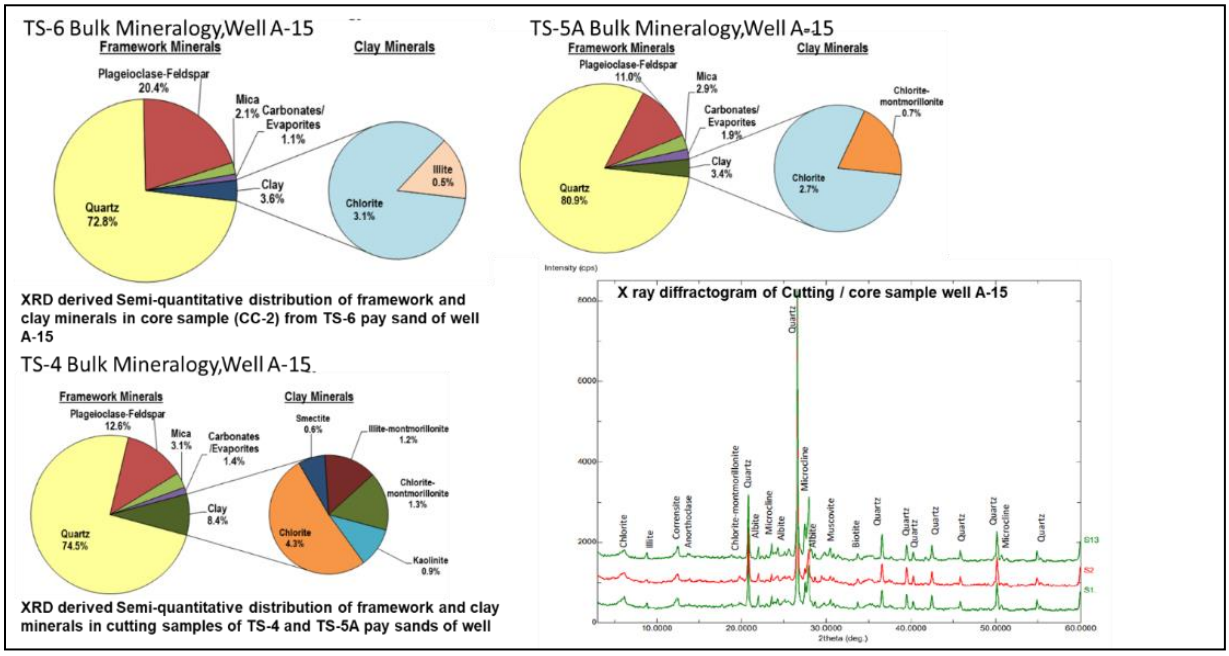

Fig. 7: Semi-quantitative distribution of bulk and clay minerals in the sample and X-ray diffractogram of Cutting / core sample well A-15

Diagenetic Events	Early → Relative time → Late
Mechanical infiltration of Clay	
Fe-oxide coating	
Mechanical compaction	
Grain dissolution & replacement	
Silica Cement	
Quartz over growth	
Authigenesis of chlorite	
Authigenesis of kaolinite	
Authigenesis of illite	
Grain deformation & fracturing	

Fig. 8: A summary of diagenetic events of the Tipam sandstones.

Bulk mineralogical breakup of core samples from pay sands of Tipam Formation.																											
Sample Deatails					Minerals (%)																						
					Felsic					Heavy						Carbonate and Evaporite				Clay							
Sample no	Well Name	Pay sand	Sample Type Cutting/Conventional Core(CC)	Depth Interval(m)	Quartz	Microcline	Albite	Anorthoclase	Muscovite	Ilmenite	Siderite	Pyrite	Limonite	Rutile	Biotite	Calcite	Dolomite	Gypsum	Barite	Kaolinite	Chlorite	Corrensite	Smectite	Illite	Glauconite	Smectite-Kaolinite	Illite-Montmorillonite	Chlorite-Montmorillonite
1	A-15	TS-4	Cutting	2865-2870	74.5	3.8	8.8	-	1.9	-	-	-	-	-	1.2	-	-	-	1.4	0.9	4.3	-	0.6	-	-	-	1.2	1.3
2	A-15	TS-5A	Cutting	2890-2900	80.9	2.1	9.0	-	1.8	-	-	-	-	-	1.0	1.2	0.7	-	-	-	2.7	-	-	-	-	-	-	0.7
3	A-98	TS-6C	Cutting	3600-3605	82.8	4.2	0.5	-	1.5	-	0.6	-	-	-	1.3	-	-	-	0.5	-	2.5	1.5	1.1	3.0	0.6	-	-	-
4	A-84	TS-4	Cutting	1935-1940	77.5	3.7	3.7	-	3.0	-	-	-	-	0.6	0.6	2.2	0.6	-	1.7	0.6	1.4	1.8	0.6	-	-	-	1.0	1.1
5	A-84	TS-3A	Cutting	1425-1430	82.0	2.6	3.1	-	1.8	-	-	0.5	-	-	1.4	1.8	-	-	0.6	-	1.1	1.8	0.5	1.6	-	-	1.1	-
6	A-151	TS-4B	Cutting	3455-3465	84.0	-	1.4	-	1.3	0.6	1.5	0.6	0.7	-	-	1.2	-	-	-	5.8	-	1.9	-	1.2	-	-	-	-
7	A-121	TS-4B	Cutting	3140-3150	72.2	3.4	1-	1.1	-	-	-	-	-	-	2.3	5.1	0.8	-	1.0	-	2.4	0.6	-	1.0	-	-	-	-
8	A-121	TS-5C	Cutting	3405-3415	79.9	4.4	8.4	-	0.8	-	-	0.5	-	0.4	0.9	-	0.7	-	1.6	-	0.4	1.3	0.7	-	-	-	-	-
9	A-121	TS-6B	Cutting	3650-3660	75.9	4.9	11.3	-	0.6	-	-	-	-	-	1.1	0.9	0.5	-	2.5	-	1.2	-	0.5	0.6	-	-	-	-
10A	AA-E	TS-5A	Cutting	3120-3130	79.2	3.9	7.6	0.7	1.0	-	-	-	-	-	0.7	-	-	-	2.2	-	0.8	1.4	-	1.6	-	-	-	0.9
10B	AA-E	TS-5A	Cutting	3120-3130	76.3	3.5	10.7	0.7	1.1	-	-	-	-	-	1.2	-	-	2.2	1.6	-	1.4	0.6	-	0.9	-	-	-	-
11	A-120	TS-3A	Cutting	2680-2690	83.9	1.3	1.6	-	2.5	-	-	-	-	-	1.0	-	-	-	0.5	-	1.4	4.1	-	3.0	-	-	-	0.7
12	A-120	TS-5	Cutting	3075-3085	80.1	2.1	9.7	-	-	-	-	-	-	-	-	1.5	-	-	2.9	-	1.9	0.9	-	1.0	-	-	-	-
13	A-15	TS-6	CC	3173.5-3178.5	72.8	8.7	11.7	-	0.8	-	-	-	-	-	1.3	-	-	-	1.1	-	3.1	-	-	0.5	-	-	-	-
14	A-12	TS-2	CC	2635-2644	88.0	2.1	4.6	-	0.5	-	-	-	-	-	1.1	-	-	-	1.9	-	-	1.2	-	0.5	-	-	-	-
15	A-105	TS-2	CC	2849-2858	74.4	1.3	9.5	-	1.6	-	-	-	-	-	-	-	-	0.7	1.2	-	-	6.8	0.7	3.9	-	-	-	-
16	A-105	TS-2	CC	2849-2858	88.2	1.5	4.7	-	0.8	-	-	-	-	-	1.0	-	-	-	0.7	-	1.0	1.2	0.4	0.4	-	-	-	-
17	A-101	TS-2	CC	2662-2671	71.7	4.8	4.3	-	2.8	-	-	0.8	-	-	-	-	0.8	1.0	1.8	0.8	0.9	3.8	-	3.8	-	0.9	-	1.8
18	A-101	TS-2	CC	2662-2671	89.7	0.5	3.8	-	0.5	-	-	-	-	-	2.1	-	-	-	1.4	-	1.6	-	0.5	-	-	-	-	-
19	A-95	TS-1	CC	2276.29-2279.29	88.3	0.8	5.3	-	-	-	-	-	-	-	1.4	-	-	-	1.9	-	-	1.0	-	0.6	-	-	-	0.6

Table 2: Bulk mineralogical breakup of core samples from sand units of Tipam Formation.